Microfluid Nanofluid (2011) 11:601–610
DOI 10.1007/s10404-011-0826-1

RESEARCH PAPER

Generation of uniform-size droplets by multistep hydrodynamic droplet division in microfluidic circuits

Tatsuru Moritani · Masumi Yamada · Minoru Seki

Received: 9 December 2010 / Accepted: 13 April 2011 / Published online: 7 June 2011
© Springer-Verlag 2011

Abstract A microfluidic system is presented to generate multiple daughter droplets from a mother droplet, by the multistep hydrodynamic division of the mother droplet at multiple branch points in a microchannel. A microchannel network designed based on the resistive circuit model enables us to control the distribution ratio of the flow rate, which dominates the division ratios of the mother droplets. We successfully generated up to 15 daughter droplets from a mother droplet with a variation in diameter of less than 2%. In addition, we examined factors affecting the division ratio, including the average fluid velocity, interfacial tension, fluid viscosity, and the distribution ratio of volumetric flow rates at a branch point. Additionally, we actively controlled the volume of the mother droplets and examined its influence on the size of the daughter droplets, demonstrating that the size of the daughter droplets was not significantly influenced by the volume of the mother droplet when the distribution ratio was properly controlled. The presented system for controlling droplet division would be available as an innovative means for preparing monodisperse emulsions from polydisperse emulsions, as well as a technique for making a microfluidic dispenser for digital microfluidics to analyze the droplet compositions.

Keywords Microfluidics · Droplet division · Monodisperse emulsion · Hydrodynamic resistance

T. Moritani · M. Yamada · M. Seki (✉)
Department of Applied Chemistry and Biotechnology, Graduate School of Engineering, Chiba University, 1-33 Yayoi-cho, Inage-ku, Chiba 263-8522, Japan
e-mail: mseki@faculty.chiba-u.jp

1 Introduction

Monodisperse emulsions or droplets are widely used not only as functional materials for drugs, foods, and cosmetics, but also as the starting materials for producing monodisperse particles and capsules for various chemical, biomedical, and industrial applications. Since conventional methods like mechanical homogenization processes usually generate polydisperse emulsions, specific techniques such as membrane emulsification should be employed to prepare monodisperse emulsions (Mine et al. 1996; Joscelyne and Tragardh 2000).

In the last decade, microfluidic devices have become a powerful means of preparing micrometer-size droplets with extremely high monodispersity and desirable sizes (Teh et al. 2008; Sugiura et al. 2001a; Nisisako et al. 2002; Haeberle et al. 2007). The generated microdroplets were utilized to prepare highly monodisperse particles or capsules (Sugiura et al. 2001b; Xu et al. 2005; Takeuchi et al. 2005; Um et al. 2008), which are generally hard to obtain when using bulk-scale techniques. Also, highly functional materials such as double emulsions (Sugiura et al. 2004; Okushima et al. 2004; Lao et al. 2009), Janus droplets and particles (Nisisako et al. 2006), and non-spherical particles (Nie et al. 2005; Dendukuri et al. 2005) were prepared using microchannel emulsification techniques. On the other hand, the ability to produce monodisperse droplets has been employed to prepare microscale chemical/biochemical reactors or containers (Song et al. 2006). For instance, droplet-based biochemical screening/analysis systems (Zheng et al. 2003; Wu et al. 2009; Joensson et al. 2009), cell-encapsulating devices (He et al. 2005; Huebner et al. 2008; Edd et al. 2008), and techniques for fusing droplets (Tan and Takeuchi 2006; Tan et al. 2007; Ahn et al. 2006; Fidalgo et al. 2007; Sivasamy et al. 2010) have been reported.

In general, various factors dominate the size of the generated droplets in microfluidic channels, including the microchannel geometries (T-shape confluence, Nisisako et al. 2002; flow focusing, Nie et al. 2008; or vertical micronozzle array, Kobayashi et al. 2008), channel size, physicochemical properties of fluids (fluid viscosity, interfacial tension, and wettability to the channel wall), and operation conditions like flow rates and temperature. Among these factors, the orifice/nozzle size is one of the most critical factors determining the droplet size, and the droplet size is not significantly changed even when the flow rates are changed. A technique for dividing mother droplets into small daughter droplets would therefore be a promising means of controlling the droplet size in microchannels. Researchers have developed microfluidic systems for splitting one droplet into several daughter droplets and controlling the division ratio, by adjusting the flow resistances of microchannels (Link et al. 2004; Menetrier-Deremble and Tabeling 2006). Also, a microfluidic system to actively control the division ratio has been proposed, by employing electrical (Link et al. 2006) or thermal (Ting et al. 2006) control, microvalve actuation (Choi et al. 2010) or a bifurcating microchannel where the distribution ratio at the branch point was controlled by introducing a continuous phase into one of the two branch channels (Yamada et al. 2008). As another example, Lao et al. (2009) have reported on a microfluidic system to generate double emulsions, in which they obtained droplets incorporating up to ten inner daughter droplets generated by multistep droplet division. Although these studies have demonstrated the promise of droplet division techniques, it is obvious that the size of the daughter droplets is determined by the volume of the mother droplets and the volumetric ratio of the divided droplets. A microfluidic system that enables the generation of daughter droplets with a constant volume, regardless of the mother droplet sizes, would therefore be highly useful. Such a system would be available as a means for producing droplets in parallel with sizes much smaller than the microchannel dimensions. Also, dispensing of a small aliquot from a microdroplet and further mixing with a reagent droplet would be possible, which allows us to analyze the droplet compositions for droplet-based chemical reaction/analysis systems. In addition, it would enable a direct decrease in the dispersity of droplet sizes of polydisperse emulsions.

Here we present a simple but efficient microfluidic system to divide the mother droplets and to generate multiple daughter droplets with constant sizes by utilizing microchannel networks having multiple branch channels with properly adjusted hydrodynamic resistances. We have previously developed a scheme called "hydrodynamic filtration" for continuous size-dependent cell/particle separation; this scheme utilizes a microchannel network composed of a main channel and multiple branch channels (Yamada and Seki 2005). The flow rate distributed into each branch channel is properly adjusted by regarding the microchannel network as a resistive circuit, which determines the maximum size of particles/cells that can go through the branch channels. By adopting this concept, we are able to control the distribution ratio of flows through the multiple branch channels, as shown in Fig. 1a. In this figure, the microchannel network consists of a main channel and multiple branch channels, as in the case of the hydrodynamic filtration scheme. A droplet flowing through the main channel is divided into two droplets at a branch point; the smaller one (daughter droplet) flows through the branch channel, while the larger (mother droplet) is further divided into two droplets at the next branch point. The size of the daughter droplet can be adjusted by controlling the ratio of the flow rate distributed into the branch channel. Proper control of the hydrodynamic resistance of the entire microchannel network regarded as a resistive circuit (Fig. 1b) would thus enable us to uniformize the division ratios at multiple branch points, achieving the formation of monodisperse daughter droplets from a mother droplet. In the experiment, we examined the factors possibly affecting the size of the generated daughter droplets, including the interfacial tension between the oil/water phases, flow velocity, the theoretical distribution ratio of flow rates, and the fluid viscosity. Also, to fully exploit the presented concept, we proposed a microfluidic device for 15-step droplet division. Furthermore, we examined the effects of the mother droplet size on the formation of the daughter droplets, by actively controlling the size of the mother droplets using a two-step droplet division system.

2 Experimental section

2.1 Microchannel design

Microchannels were designed based on the resistive-circuit analogy of the whole microchannel network as shown in Fig. 1b. When a uniform Newtonian fluid is continuously flowing through a microchannel having multiple branch points and branch channels, the volumetric flow rates distributed to the main/branch channels are determined by the hydrodynamic resistances of the microchannel networks. The hydrodynamic resistance R of a rectangular microchannel segment with a uniform depth and width is expressed as follows:

$$R = \frac{12\mu L}{l_1^3 l_2}\left[1 - \frac{192 l_1}{\pi^5 l_2}\sum_{n=1,3,5}^{\infty}\frac{\tanh(n\pi l_2/2l_1)}{n^5}\right]^{-1} \quad (1)$$

where L is the length of the microchannel segment, l_1 and l_2 are either the width or depth of the microchannel (l_1 is the

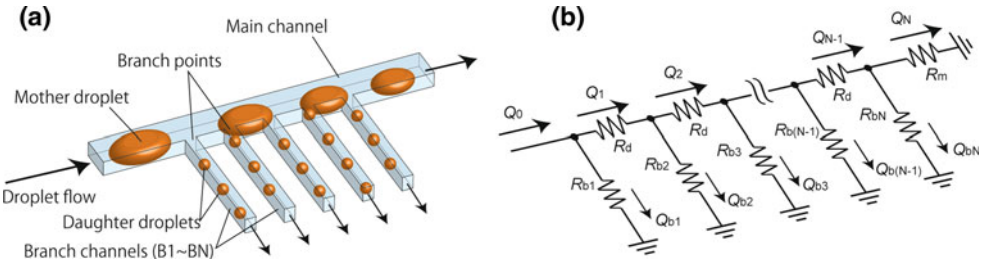

Fig. 1 **a** Schematic image showing the microfluidic network for generating multiple daughter droplets by multistep droplet division and **b** corresponding resistive circuit model

larger of these two values), and μ is the fluid viscosity (Constantinescu 1995). Considering that R is analogous to the resistance in an electric circuit, the distribution ratio of the flow rates could theoretically be calculated by using Ohm's law, where the volumetric flow rate Q and the pressure drop ΔP correspond to the current I and voltage V, respectively; Q_{bn} is determined by the initial values of the flow rate Q_0 and the hydrodynamic resistances R of the microchannel segments composing the entire channel network. Here the theoretical distribution ratio of the flow rate, α_n, is defined as the ratio of the volumetric flow rate split into a branch channel n, $Q_{\mathrm{b}n}$, to the total flow rate introduced into the microchannels, Q_n, and is expressed as follows:

$$\alpha_n = Q_{\mathrm{b}n}/Q_0 \tag{2}$$

In addition, the division ratio of the flow rate at a branch point is defined as follows:

$$\beta_n = Q_{\mathrm{b}n}/(Q_n + Q_{\mathrm{b}n}) = Q_{\mathrm{b}n}/Q_{n-1} \tag{3}$$

Although the actual flow profile in the two-phase segmented flow system, as shown in Fig. 1a, is nonuniform and highly complicated, and the hydrodynamic resistance would be higher than that of the uniform flow system (Adzima and Velankar 2006; Sessoms et al. 2009), we determined the theoretical distribution ratio α and the division ratio β, assuming that the viscosity μ is uniform. For example, the value of β_N (β_n at the last branch point) in Fig. 1b is expressed by the following equation:

$$\beta_N = Q_{\mathrm{b}N}/(Q_N + Q_{\mathrm{b}N}) = R_{\mathrm{m}}/(R_{\mathrm{m}} + R_{\mathrm{b}N}) \tag{4}$$

since the ratio of the volumetric flow rates at the branch point is inversely proportional to the ratio of the hydrodynamic resistances of the main/branch channels, which is shown as follows:

$$Q_N : Q_{\mathrm{b}N} = 1/R_{\mathrm{m}} : 1/R_{\mathrm{b}N} \tag{5}$$

2.2 Materials

Olive oil and sorbitan monooleate (Span 80) were obtained from Wako Pure Chemical Ind., Ltd. (Osaka, Japan). Dextran from *Leuconostoc* spp. (Mr = ~500,000) was obtained from Sigma-Aldrich Corp. (St Louis, MO, USA). Polydimethylsiloxane (PDMS; Sylpot 184) was obtained from Dow Corning Toray Corp. (Tokyo, Japan). All other chemicals were of analytical grade. The viscosities of olive oil and deionized water were 81 and 0.89 mPa s at 25°C, respectively, as measured by using a viscometer.

2.3 Microfluidic experiments

PDMS microdevices were fabricated using the usual soft lithography and replica molding techniques (Duffy et al. 1998). Negative photoresist (SU-8) structures were initially patterned on a silicon wafer, and a PDMS replica having microchannel structures was obtained using the patterned mold. The PDMS replica was bonded with a flat PDMS plate after O_2 plasma treatment. The width of the branch channels was 25 μm for all microdevices, while that of the main channel was either 100 or 50 μm. The channel depth was uniform for all devices, 20 μm. Both the continuous oil phase and the dispersed water phase were introduced into the microchannel using syringe pumps (KDS250, KD Scientific, Holliston, MA, USA). To form monodisperse mother droplets, a T-shape confluence was employed. The droplet behaviors were observed using an inverted microscope (IX70, Olympus, Tokyo, Japan) and a high-speed CCD camera (VCC-H1000, Digimo Corp., Osaka, Japan). The droplet volumes were calculated from the obtained images; we analyzed the areas of droplets, and assumed a spherical or ellipsoidal shape when the droplet width was smaller than the channel width. When the droplet width was (almost) equal to the channel width, we calculated the droplet size by measuring the length and the area, and by regarding the droplet shape composed of an elliptic cylinder and two hemispheres of an ellipsoid. On average, the volumes and sizes of ~50 droplets were calculated for each condition.

3 Results and discussion

3.1 Generation of daughter droplets by multistep droplet division

In order to divide the mother droplets and generate daughter droplets with uniform sizes at multiple branch

points, two schemes are available: (1) equal division-ratio scheme and (2) equal distribution-ratio scheme. In the first scheme, the division ratios β_1–β_N at the branch points B1–BN are equal, while in the second scheme, the distribution ratios α_1–α_N are equal. We first examined the equal division-ratio scheme using a microfluidic network having five branch channels with main/branch channel widths of 100 and 25 μm, respectively. The theoretical division ratio β was 0.1 for all branch channels, i.e., $Q_{bn} = 0.1 \times 0.9^{n-1} \times Q_0$ for $n = 1$ to 5. As a result, however, the diameters of the daughter droplets D_d were not uniform; the daughter droplets generated at the downstream branch points were much smaller than those generated at the upstream branch points (data not shown).

We next examined the equal distribution-ratio scheme using a microfluidic network having five branch channels as shown in Fig. 2a, where α_n was 0.1 for all branch channels, i.e., $Q_{bn} = 0.1 \times Q_0$. Branch channels B1–B5 were composed of narrow (width 25 μm; length 6.04–5.48 mm) and wide (width 100 μm; length 0–0.56 mm) segments, to properly adjust the hydrodynamic resistances while keeping the uniform lengths. Figure 2b shows a microscopic image of the generated daughter droplets, when the olive oil and distilled water were, respectively, introduced as continuous and disperse phases, with an equal flow rate of 60 μl h^{-1}. At the confluence point, mother droplets with a volume of ~500 pl were generated at a frequency of ~30 droplets s^{-1}. When the head of a mother droplet just passed through a branch point, a daughter droplet started to generate, and the daughter was separated from the tail of the mother droplet, which flowed into the branch channel; one daughter droplet was accurately generated from a mother at each branch point. In contrast to the equal division-ratio scheme, the sizes of the generated daughter droplets were much more uniform, as shown in Fig. 2b; the diameters of the daughter droplets D_d were 23–27 μm. However, the sizes of the daughter droplets flowing through branch channels B1 and B2 were ~20 and ~10% smaller than those flowing through B3–B5, respectively. This non-uniformity in the daughter droplet size was due to the tail position of the mother droplets at the first two branch points, where the droplet tails were separated from the lower sidewall at the time of droplet division.

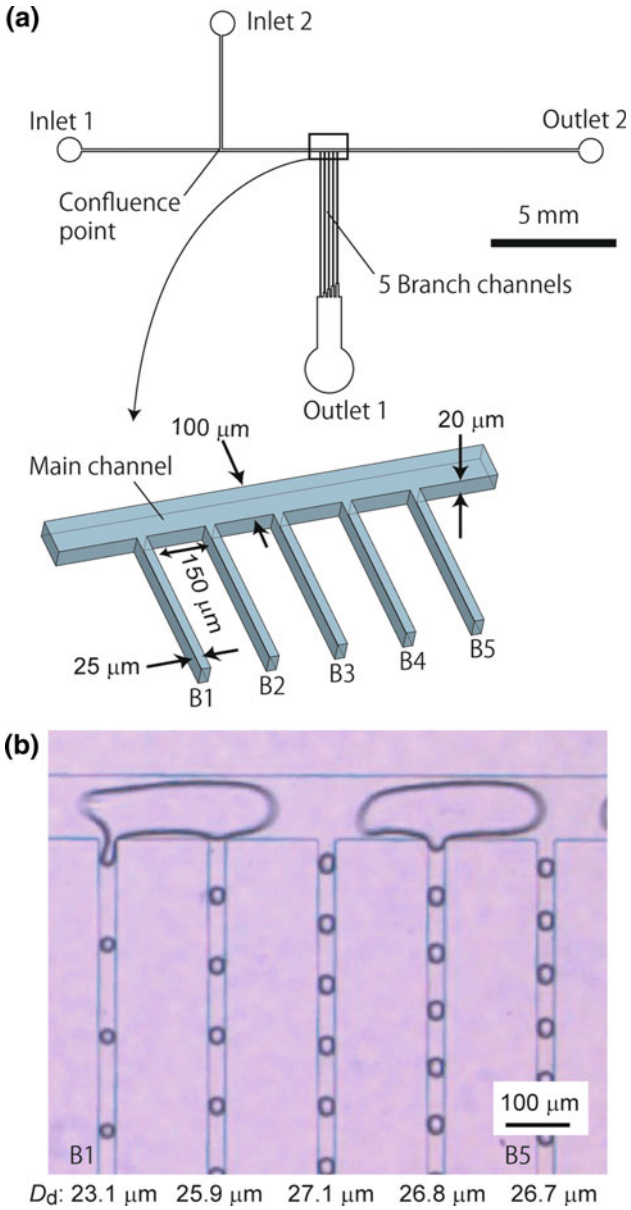

Fig. 2 **a** A schematic image showing the microchannel design having five branch channels and its detailed structure, and **b** a micrograph showing the mother droplets flowing through the main channel and the daughter droplets generated at the branch points and flowing in the branch channels

To improve the uniformity of the daughter droplet sizes, we designed and fabricated a microchannel network, as shown in Fig. 3a, which was equipped with two drain channels (D1 and D2). These drain channels were connected to Outlet 1, which had smaller distribution ratios α (=0.05) than those for branch channels B1–B5 (α_1–$\alpha_5 = 0.1$). In addition, the width of the main channel was decreased from 100 to 50 μm at the region connected with the branch/drain channels, to effectively push the tails of the mother droplets against the channel wall at the time of droplet division. Figure 3b shows the generated daughter droplets at the branch points and flowing through branch channels B1–B5, under the same operation condition as those shown in Fig. 2b. At the two branch points to the drain channels D1 and D2, the tail of the mother droplet was pushed against the lower sidewall, and daughter droplets were not generated because of the small distribution ratio α, while only the continuous oil phase was removed through these drain channels. On the other hand, mother droplets were divided and daughters were

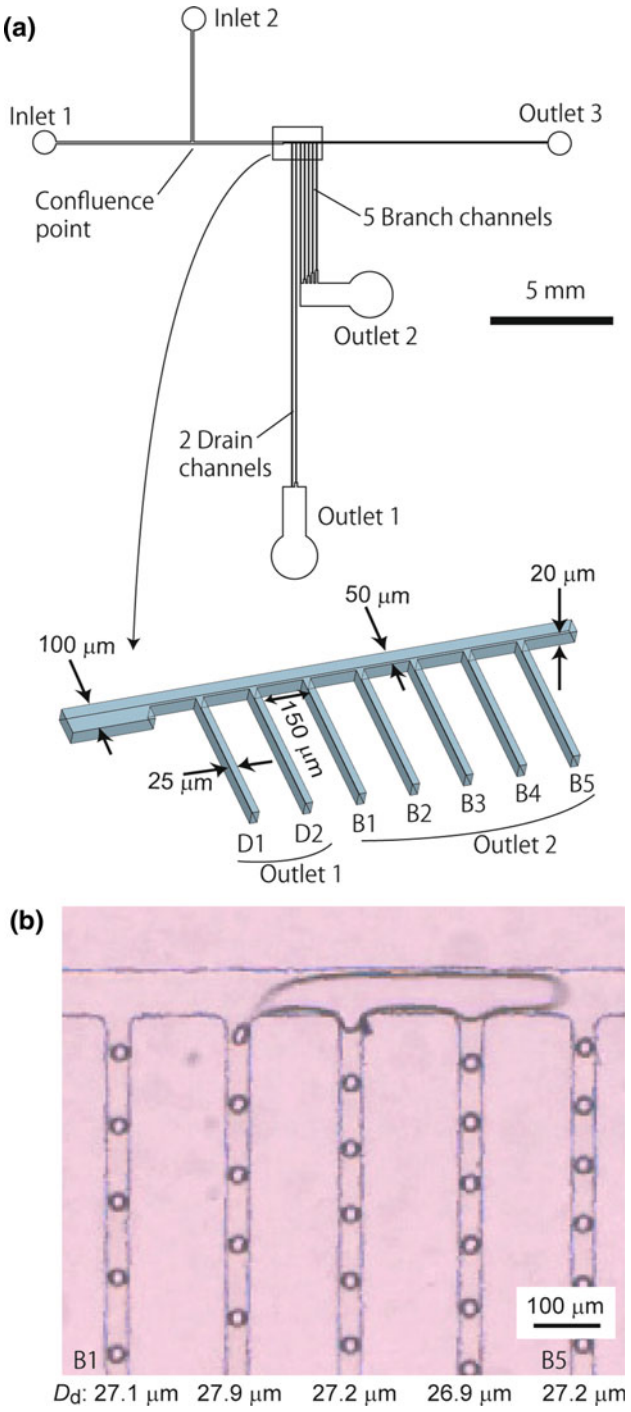

Fig. 3 **a** Schematic images showing the microchannel design having two drain channels and five branch channels, and **b** a micrograph showing the mother droplets flowing through the main channel and the daughter droplets generated at the branch points and flowing in the branch channels

generated at the branch points B1–B5, with a highly uniform value of D_d. The individual CV (coefficient of variation) value of D_d, which was defined as the standard deviation divided by the mean value of the droplet diameter, was 1.6–1.8% for each branch channel, while the total CV value of D_d for five branch channels was 1.7%, showing high uniformity in the diameters of the daughter droplets. The experimental ratios of distribution ratios α, which were estimated from the interval of the flowing daughter droplets, were 0.045–0.037 for branch channels B1–B5, despite the theoretical distribution ratio α being 0.1. This discrepancy in theoretical and experimental values of distribution ratios was due to the increased fluid resistance in the two-phase droplet flow compared to the uniform laminar flow systems (Adzima and Velankar 2006). From these results, we confirmed that the tail position of the mother droplets is critical to generating uniform-size daughter droplets. The equal distribution-ratio scheme was therefore employed in all the following experiments.

3.2 Factors affecting the size of daughter droplets

Various factors would affect the size of the daughter droplets generated by the presented scheme of multistep droplet division, including the microchannel geometries, physical characteristics of fluids, and operation conditions. We examined the effects of four factors that possibly affect the size of the daughter droplets; the distribution ratio α, interfacial tension between the continuous/dispersed phases, flow velocity, and the relative viscosities of two phases. We employed microchannel networks having three branch channels, with a main channel width of 100 μm. The diameters of the daughter droplets D_d generated at the third branch point and flowing through branch channel B3 were analyzed from the captured images. In the following experiments, the volumes of the mother droplets generated at the T-shape confluence were in the range of 500–1000 pl; the mother droplets flowing in the main channel were not spherical and the droplet width was almost equal to the width of the main channel.

First, the theoretical distribution ratio, α, was changed using seven types of microfluidic devices having three branch channels with different hydrodynamic resistances. The distribution ratios α_1 and α_2 for branch channels B1 and B2, respectively, were kept constant (0.1) for all devices, while α_3 was changed from 0.05 to 0.3. Figure 4a shows the diameter of the generated daughter droplets D_d, assuming a spherical droplet shape, and the volume ratio of the mother and daughter droplets V_d/V_m when α was changed. The effect of the interfacial tension between the oil and the water phases was also examined by adding 1.0% (w/w) Span 80 in the continuous oil phase; the interfacial tensions were 22.9 and 4.8 mN m^{-1} when the concentrations of Span 80 were 0 and 1.0% (w/w), respectively. Without adding Span 80, daughter droplets were not generated when α was lower than 0.1, because of the relatively high interfacial tension between the oil and the water

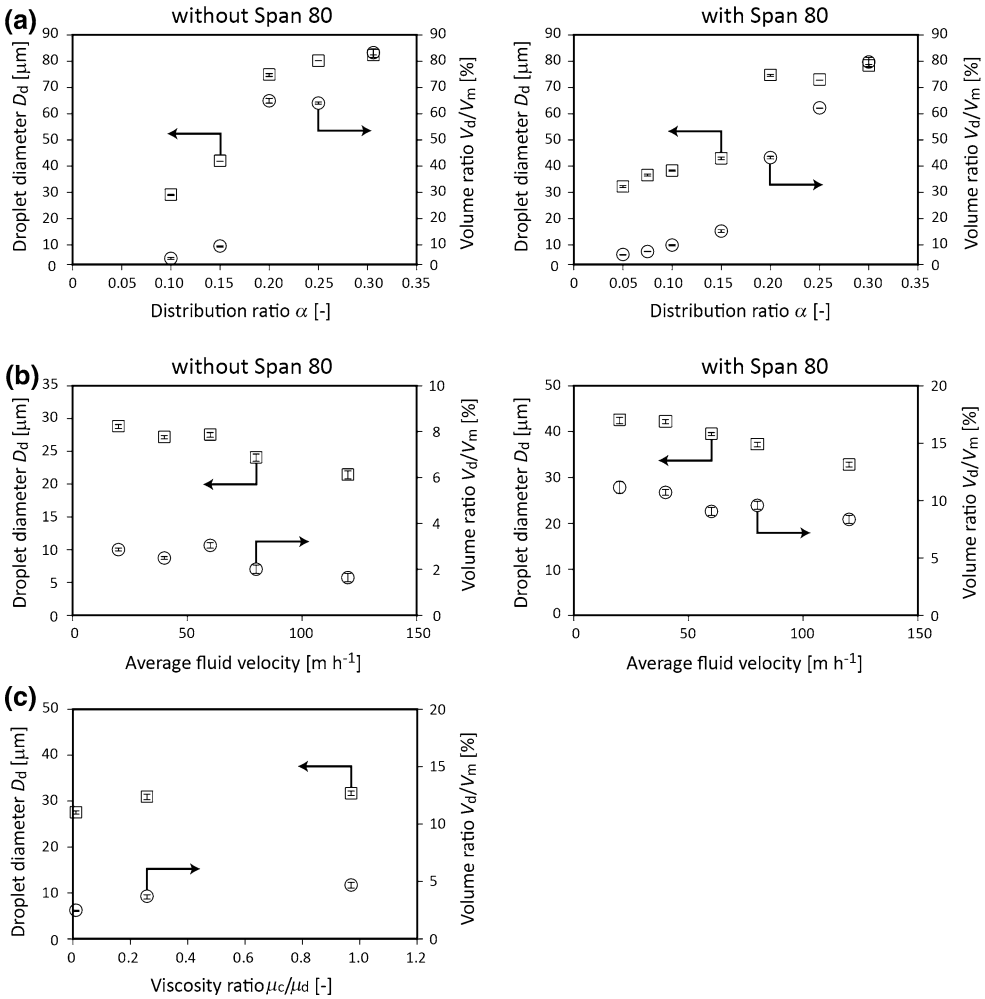

Fig. 4 Effects of parameters affecting the generation of daughter droplets. **a** Effect of the distribution ratio α and the presence of the surfactant (1.0% Span 80), **b** effect of the average fluid velocity, and **c** effect of the viscosity ratio, on the formation of daughter droplets. D_d, diameter of daughter droplets; V_d, volume of the daughter droplets; V_m, volume of the mother droplets; μ_c, viscosity of continuous phase; μ_d, viscosity of the disperse phase. All data show the mean ± SD of at least 30 droplets

phases. When α was higher than 0.2, the diameter D_d and the volume ratio V_d/V_m of the daughter droplets increased dramatically, and the size of the daughter droplets became more than half that of the mother droplet volumes. These results indicate that the distribution ratio α in the presented microsystem should be in the range of 0.1–0.15 to achieve multistep division of droplets, when the interfacial tension is relatively high. On the other hand, the lower interfacial tension achieved a generation of daughter droplets even when α was lower than 0.1. The volume ratio of the daughter/mother droplets, V_d/V_m, was almost equal to the distribution ratio α, when α was lower than 0.15. The formation of the daughter droplets in the low α value conditions can be attributed to the decrease in the Laplace pressure (Aota et al. 2007) at the oil–water interface formed at the entrance of the branch channel. The Laplace pressure works as friction for droplets entering the narrow branch channel, which is expressed by the following equation:

$$\Delta P = \gamma / R \tag{6}$$

where ΔP is the pressure difference at the interface, γ is the interfacial tension, and R is the curvature radius. In the lower interfacial-tension condition, the Laplace pressure was decreased, resulting in the larger volume of daughter droplets entering the branch channel at the moment of droplet division.

The fluid velocity would also affect the size of the daughter droplets. The effect of average fluid velocity was examined by changing the inlet flow rates while keeping the ratio of water/oil flow rates constant, 1:1, using a branch channel (the third channel) with the α value of 0.1. Figure 4b shows the relation between the diameter of the daughter droplets D_d and the average fluid velocity in the main channel just before passing the first branch points. As a result, D_d decreased with increases in the average fluid velocity, regardless of the addition of Span 80 in the oil phase. The volume ratios, V_d/V_m, were 3–2% and 11–8% for the high and low interfacial-tension conditions, respectively, although the theoretical distribution ratio α was 0.1. When the flow velocity was high, the tail of the

mother droplet was separate from the channel wall even at the third branch point, resulting in the generated daughter droplets being relatively small. The high fluid velocity possibly enhanced the secondary flow inside the droplets and in the continuous phase between the droplets, shifting the tail position of the mother droplets toward the channel center. It was thus suggested that the tail position of droplets, not the fluidic shear stress, is a critical factor in controlling the size of the generated daughter droplets.

Finally, we examined the effects of the relative fluid viscosity of the disperse water phase (μ_d) to the continuous oil phase (μ_c), by adding dextran (Mr = ~500,000) into the water phase; μ_d was changed from 0.89 to 78.2 mPas, with μ_d/μ_c value being changed from 0.011 to 0.97. As a result, D_d slightly increased with the increase of the viscosity of the water phase, although its effect was not significant, as shown in Fig. 4c.

3.3 15-Step droplet division by supplying continuous phase

As shown in the experimental results, shown in Fig. 4a, the optimal distribution ratio α should be 0.1–0.15 when the interfacial tension is relatively high. However, since the relative volume of daughter droplets to mother droplets, V_d/V_m, was much smaller than α, the maximum number of division steps should be lower than ~7 when α is 0.1; we observed the coalescence of mother droplets due to the lack of the continuous phase when a microchannel for 10-step droplet division was employed (data not shown). To increase the number of division steps and the number of generated daughter droplets from a mother droplet, we designed and fabricated a microchannel network, as shown in Fig. 5a. This microchannel network was equipped with 15 branch channels, two drain channels, one inlet (Inlet 2) for the dispersed water phase, and three inlets (Inlets 1, 3, and 4) for the continuous oil phase, to achieve an adequate supply for the continuous phase. Inlet channels 3 and 4 were connected to the main channel at the points between branch channels B5 and B6, and B10 and B11, respectively. The theoretical distribution ratio α for each branch channel (B1–B15) was 0.1, while that for the drain channels (D1 and D2) was 0.05, when the ratio of flow rates from Inlets 1, 3, and 4 was 10: 6: 5. These values were determined based on the resistive circuit model to achieve a uniform value of α for 15 branch channels. As is the case for the microdevice shown in Fig. 3, two drain channels were responsible for pushing the tail position of the mother droplets toward the lower sidewall in the main channel. Also, the microchannel width was changed from 100 to 50 μm just before passing through the branch points.

Figure 5b–d shows the generated daughter droplets, and Fig. 5e shows the diameter of daughter droplets D_d, when olive oil without Span 80 was introduced from Inlets 1, 3, and 4 at flow rates of 30, 18, and 15 μl h^{-1}, respectively. The water flow rate from Inlet 2 was 30 μl h^{-1}. Although the size of the daughter droplets slightly increased with increases in the branch-channel number, almost uniform-size droplets were obtained with the entire CV value for droplet diameter being 1.9%. It was confirmed that introduction of the continuous oil phase between the flowing droplets prevented the mother droplets from coalescing with each other. The sum of the volumes of 15 daughter droplets was ~40% of the volume of one mother droplet, and thus, a further increase in the step number would be possible using a microchannel network having a larger number of inlets and branch channels.

3.4 Effect of mother droplet size

The presented system for droplet division would be useful if it would work to convert multiple-size droplets into monodisperse emulsions. Although we examined the factors affecting the size of the daughter droplets, it is

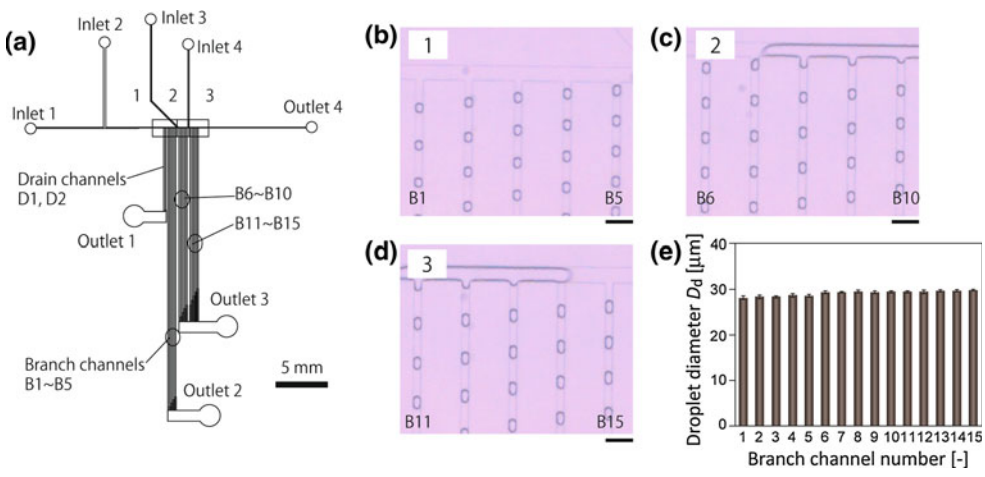

Fig. 5 Demonstration of 15-step droplet division by supplying continuous phase from multiple inlets. **a** Microchannel design, **b**, **c** droplets flowing through the branch channels B1–B15, and **e** size distribution of daughter droplets flowing through the branch channels B1–B15. **b**, **c**, and **d** correspond to the areas 1, 2, and 3 shown in (**a**), respectively

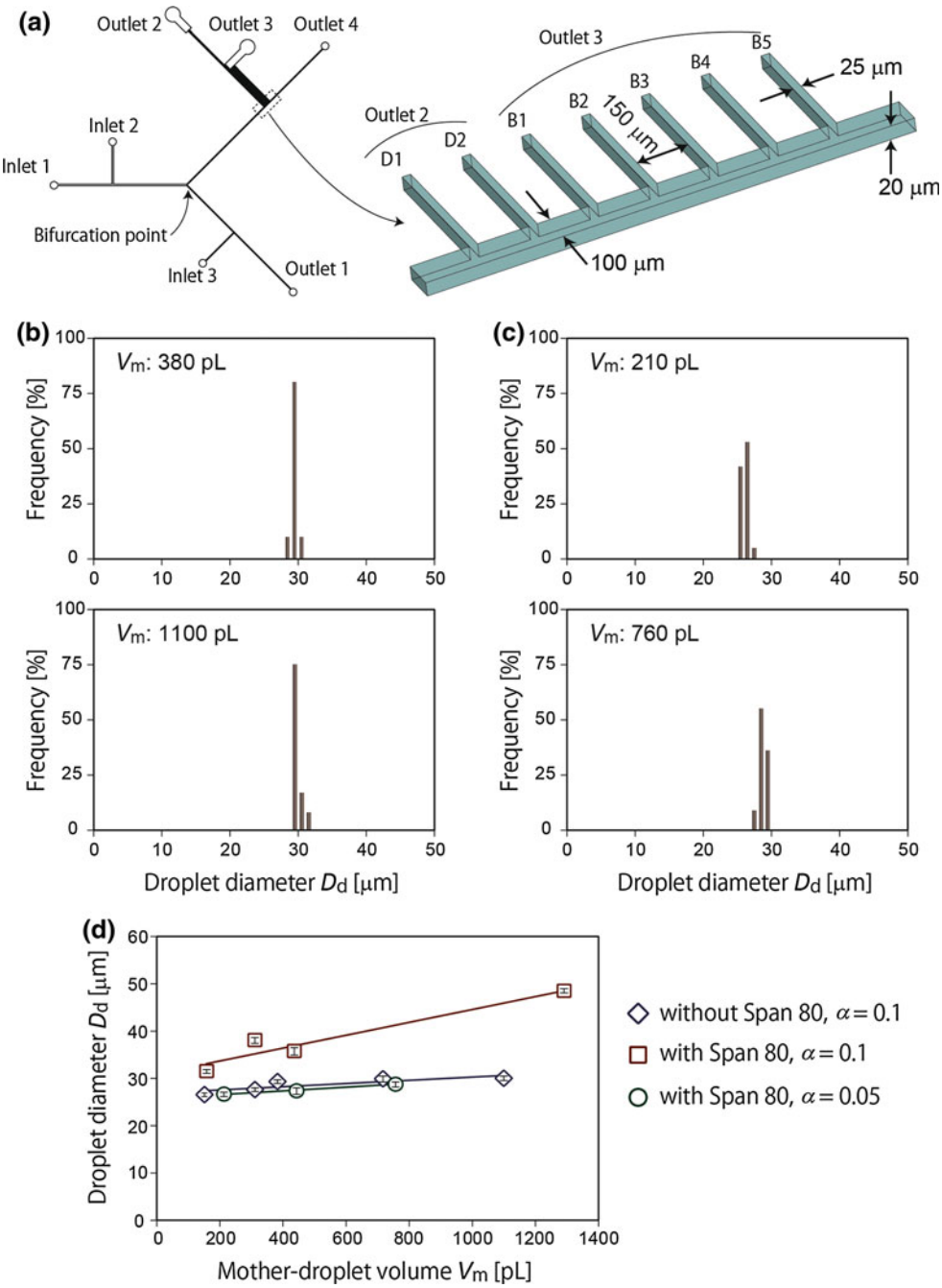

Fig. 6 Examination of the effects of mother droplet size on the formation of daughter droplets. **a** Microchannel design for dynamically controlling the mother droplet size by dividing mother droplets into two droplets at the bifurcation point and generating the five daughter droplets. **b**, **c** the size distribution of daughter droplets when the mother droplet volumes were changed as indicated. In (**b**), the distribution ratio α was 0.1 and Span 80 was not used, while in (**b**), α was 0.05 and Span 80 was added (1.0%) in the continuous oil phase. **d** Effects of the mother droplet size on the diameter of the generated daughter droplets D_d

necessary to directly investigate the effect of the mother droplet size. Since it was difficult to widely change the size of the mother droplets without changing the microchannel dimensions and operation conditions when a passive microchannel system is used, we employed a microchannel as shown in Fig. 6a, which enables active control of the mother droplet size. In this device, mother droplets generated at the T-shape confluence were divided into two smaller-size mother droplets at the bifurcation point, when the flow rate of the continuous phase from Inlet 3 (tuning flow) was relatively low. When the tuning flow rate was sufficiently high, the mother droplets were not divided and they were introduced into the upper branch channel. The division ratio could be accurately controlled, and we could therefore obtain droplets with different sizes (Yamada et al. 2008). One of the two generated droplets was further divided into five daughter droplets in the upper branch channel having five branch channels and two drain channels as in the microdevice shown in Fig. 3. Several types of microchannels were fabricated with different inlet-channel widths to widely control the initial size of the mother droplets. Also, microchannels with different distribution

ratios α were prepared; α for the branch (drain) channels D1 and D2 was 0.05, while that for the branch channels B1–B5 was changed either at 0.1 or 0.05.

We introduced the continuous phase from Inlets 1 and 3, and the disperse phase from Inlet 2. The flow rates from Inlets 1 and 2 were same and controlled from 30 to 60 μl h^{-1}, while the tuning flow rate from Inlet 3 was changed from 0 to 60 μl h^{-1}. As a result, mother droplets with initial volumes of 400–1350 pl were generated at the T-shape confluence, and they were divided into two smaller mother droplets at the Y-shaped bifurcation point. Otherwise, mother droplets were not divided but just introduced into the upper branch channel, when the tuning flow rate from Inlet 3 was sufficiently high.

The sizes of the formed daughter droplets through the branch channels B1–B5 and recovered from Outlet 3 are shown in Fig. 6b–d. When Span 80 was not added in the oil phase, the interfacial tension was relatively high, and the distribution ratio α was 0.1, daughter droplets with diameters of ~30 μm were generated at the branch points B1–B5. The size of the generated daughter droplets was almost constant, even when the mother droplet volume was changed from 170 to 1100 pl. On the other hand, when Span 80 was added in the oil phase and α was 0.1, the size of the daughter droplets increased with increased mother droplet size. To obtain uniform-size daughter droplets in the case of this low interfacial-tension condition, we needed to decrease the distribution ratio α from 0.1 to 0.05. As shown in Fig. 6c, d, the size of the daughter droplets did not show significant change, even when the size of the mother droplets was changed from 200 to 750 pl. These results demonstrated that a smaller value of the distribution ratio α would be better for obtaining uniform-size daughter droplets without being influenced by the mother droplet sizes, on the condition that daughter droplets are generated by the division of mother droplets. The previous study by Lao et al. (2009) has demonstrated the multistep droplet division at a low-interfacial condition, but the size of the daughter droplets was critically dominated by the mother droplet size. While in this study, we successfully showed a strategy to generate constant-volume daughter droplets, by adjusting the distribution ratio α depending on the interfacial tension between the water and the oil phases. The presented system would therefore be applicable to preparing uniform-size droplets from polydisperse emulsions, since the initial size of the mother droplets did not significantly affect the size of the daughter droplets.

4 Conclusions

A new microfluidic system is presented to generate multiple daughter droplets from a mother droplet without the influence of the mother droplet size. We were able to produce monodisperse daughter droplets with CV values of 1.6–1.8%, and successfully generated up to 15 droplets from a mother droplet. Additionally, we examined factors that affect the size of the daughter droplets, and found that the generation of daughter droplets whose size is independent of the mother droplet size is possible, when we properly adjust the distribution ratio α depending on the interfacial tension. The presented system will likely become a useful tool not only for generating monodisperse emulsions but also for splitting microfluidic droplets to analyze the compositions of droplets containing chemical/biological substances.

Acknowledgments This research was supported in part by Grants-in-aid for Scientific Research A (20241031) from Japan Society for Promotion of Science (JSPS), and for Improvement of Research Environment for Young Researchers from Japan Science and Technology Agency (JST).

References

Adzima BJ, Velankar SS (2006) Pressure drops for droplet flows in microfluidic channels. J Micromech Microeng 16:1504–1510

Ahn K, Agresti J, Chong H, Marquez M, Weitz DA (2006) Electrocoalescence of drops synchronized by size-dependent flow in microfluidic channels. Appl Phys Lett 88:264105

Aota A, Hibara A, Kitamori T (2007) Pressure balance at the liquid-liquid interface of micro countercurrent flows in microchips. Anal Chem 79:3919–3924

Choi JH, Lee SK, Lim JM, Yang SM, Yi GR (2010) Designed pneumatic valve actuators for controlled droplet breakup and generation. Lab Chip 10:456–461

Constantinescu VN (1995) Laminar viscous flow. Springer, New York, pp 109–137

Dendukuri D, Tsoi K, Hatton TA, Doyle PS (2005) Controlled synthesis of nonspherical microparticles using microfluidics. Langmuir 21:2113–2116

Duffy DC, McDonald JC, Schueller OJA, Whitesides GM (1998) Rapid prototyping of microfluidic systems in poly(dimethylsiloxane). Anal Chem 70:4974–4984

Edd JF, Di Carlo D, Humphry KJ, Koster S, Irimia D, Weitz DA, Toner M (2008) Controlled encapsulation of single-cells into monodisperse picolitre drops. Lab Chip 8:1262–1264

Fidalgo LM, Abell C, Huck WTS (2007) Surface-induced droplet fusion in microfluidic devices. Lab Chip 7:984–986

Haeberle S, Zengerle R, Ducree J (2007) Centrifugal generation and manipulation of droplet emulsions. Microfluid Nanofluid 3:65–75

He M, Edgar JS, Jeffries GDM, Lorenz RM, Shelby JP, Chiu DT (2005) Selective encapsulation of single cells and subcellular organelles into picoliter- and femtoliter-volume droplets. Anal Chem 77:1539–1544

Huebner A, Olguin LF, Bratton D, Whyte G, Huck WTS, De Mello AJ, Edel JB, Abell C, Hollfelder F (2008) Development of quantitative cell-based enzyme assays in microdroplets. Anal Chem 80:3890–3896

Joensson HN, Samuels ML, Brouzes ER, Medkova M, Uhlen M, Link DR, Andersson-Svahn H (2009) Detection and analysis of low-abundance cell-surface biomarkers using enzymatic amplification in microfluidic droplets. Angew Chem Int Ed 48:2518–2521

Joscelyne SM, Tragardh G (2000) Membrane emulsification—a literature review. J Membr Sci 169:107–117

Kobayashi I, Takano T, Maeda R, Wada Y, Uemura K, Nakajima M (2008) Straight-through microchannel devices for generating monodisperse emulsion droplets several microns in size. Microfluid Nanofluid 4:167–177

Lao KL, Wang JH, Lee GB (2009) A microfluidic platform for formation of double-emulsion droplets. Microfluid Nanofluid 7:709–719

Link DR, Anna SL, Weitz DA, Stone HA (2004) Geometrically mediated breakup of drops in microfluidic devices. Phys Rev Lett 92:054503

Link DR, Grasland-Mongrain E, Duri A, Sarrazin F, Cheng Z, Cristobal G, Marquez M, Weitz DA (2006) Electric control of droplets in microfluidic devices. Angew Chem Int Ed 45:2556–2560

Menetrier-Deremble L, Tabeling P (2006) Droplet breakup in microfluidic junctions of arbitrary angles. Phys Rev E 74:035303

Mine Y, Shimizu M, Nakashima T (1996) Preparation and stabilization of simple and multiple emulsions using a microporous glass membrane. Colloids Surf B 6:104–112

Nie Z, Xu S, Seo M, Lewis PC, Kumacheva E (2005) Polymer particles with various shapes and morphologies produced in continuous microfluidic reactors. J Am Chem Soc 127:8058–8063

Nie Z, Seo M, Xu S, Lewis PC, Mok M, Kumacheva E, Whitesides GM, Garstecki P, Stone HA (2008) Emulsification in a microfluidic flow-focusing device: effect of the viscosities of the liquids. Microfluid Nanofluid 5:585–594

Nisisako T, Torii T, Higuchi T (2002) Droplet formation in a microchannel network. Lab Chip 2:24–26

Nisisako T, Torii T, Takahishi T, Takizawa Y (2006) Synthesis of monodisperse bicolored janus particles with electrical anisotropy using a microfluidic co-flow system. Adv Mater 18:1152–1156

Okushima S, Nisisako T, Torii T, Higuchi T (2004) Controlled production of monodisperse double emulsions by two-step droplet breakup in microfluidic devices. Langmuir 20:9905–9908

Sessoms DA, Belloul M, Engl W, Roche M, Courbin L, Panizza P (2009) Droplet motion in microfluidic networks: hydrodynamic interactions and pressure-drop measurements. Phys Rev E 80:016317

Sivasamy J, Chim YC, Wong TN, Nguyen NT, Yobas L (2010) Reliable addition of reagents into microfluidic droplets. Microfluid Nanofluid 8:409–416

Song H, Chen DL, Ismagilov RF (2006) Reactions in droplets in microfluidic channels. Angew Chem Int Ed 45:7336–7356

Sugiura S, Nakajima M, Iwamoto S, Seki M (2001a) Interfacial tension driven monodispersed droplet formation from microfabricated channel array. Langmuir 17:5562–5566

Sugiura S, Nakajima M, Itou H, Seki M (2001b) Synthesis of polymeric microspheres with narrow size distributions employing microchannel emulsification. Macromol Rapid Commun 22:773–778

Sugiura S, Nakajima M, Yamamoto K, Iwamoto S, Oda T, Satake M, Seki M (2004) Preparation characteristics of water-in-oil-in-water multiple emulsions using microchannel emulsification. J Colloid Interf Sci 270:221–228

Takeuchi S, Garstecki P, Weibel DB, Whitesides GM (2005) An axisymmetric flow-focusing microfluidic device. Adv Mater 17:1067–1072

Tan WH, Takeuchi S (2006) Timing controllable electrofusion device for aqueous droplet-based microreactors. Lab Chip 6:757–763

Tan YC, Ho YL, Lee AP (2007) Droplet coalescence by geometrically mediated flow in microfluidic channels. Microfluid Nanofluid 3:495–499

Teh SY, Lin R, Hung LH, Lee AP (2008) Droplet microfluidics. Lab Chip 8:198–220

Ting TH, Yap YF, Nguyen NT, Wong TN, Chai JCK, Yobas L (2006) Thermally mediated breakup of drops in microchannels. Appl Phys Lett 89:234101

Um E, Lee DS, Pyo HB, Park JK (2008) Continuous generation of hydrogel beads and encapsulation of biological materials using a microfluidic droplet-merging channel. Microfluid Nanofluid 5:541–549

Wu N, Zhu Y, Brown S, Oakeshott J, Peat TS, Surjadi R, Easton C, Leech PW, Sexton BA (2009) A PMMA microfluidic droplet platform for in vitro protein expression using crude *E. coli* S30 extract. Lab Chip 9:3391–3398

Xu S, Nie Z, Seo M, Lewis P, Kumacheva E, Stone HA, Garstecki P, Weibel DB, Gitlin I, Whitesides GM (2005) Generation of monodisperse particles by using microfluidics: control over size, shape, and composition. Angew Chem Int Ed 44:724–728

Yamada M, Seki M (2005) Hydrodynamic filtration for on-chip particle concentration and classification utilizing microfluidics. Lab Chip 5:1233–1239

Yamada M, Doi S, Maenaka H, Yasuda M, Seki M (2008) Hydrodynamic control of droplet division in bifurcating microchannel and its application to particle synthesis. J Colloid Interf Sci 321:401–407

Zheng B, Roach LS, Ismagilov RF (2003) Screening of protein crystallization conditions on a microfluidic chip using nanoliter-size droplets. J Am Chem Soc 125:11170–11171